JEE Journal of Ecological Engineering

Journal of Ecological Engineering 2022, 23(12), 1–13
https://doi.org/10.12911/22998993/154770
ISSN 2299–8993, License CC-BY 4.0

Received: 2022.09.06
Accepted: 2022.10.13
Published: 2022.11.01

Fabrication and Characterization of Polyphenylsulfone/Titanium Oxide Nanocomposite Membranes for Oily Wastewater Treatment

Thaer Al-Jadir[1*], Saja Mohsen Alardhi[2], Mustafa A. Alheety[3], Aya A. Najim[4], Issam K. Salih[5], Mustafa Al-Furaiji[6], Qusay F. Alsalhy[7]

[1] Environment Research Center, University of Technology-Iraq, Baghdad, Iraq
[2] Nanotechnology and Advanced Materials Research Center, University of Technology-Iraq, Baghdad, Iraq
[3] Department of Nursing, Al-Hadi University College, Baghdad, Iraq
[4] Department of Environmental Engineering, University of Baghdad, Baghdad, Iraq
[5] Department of Chemical Engineering and Petroleum Industries, Al-Mustaqbal University College, Babylon, Iraq
[6] Environment and Water Directorate, Ministry of Science and Technology, Baghdad, Iraq
[7] Membrane Technology Research Unit, Department of Chemical Engineering, University of Technology-Iraq, Baghdad, Iraq
* Corresponding author's e-mail: 150046@uotechnology.edu.iq

ABSTRACT

Polyphenylsulfone (PPSU) membranes are critical for numerous applications, including water treatment, oil separation, energy production, electronic manufacturing, and biomedicine because of their low cost; regulated crystallinity; and chemical, thermal, and mechanical stability. Numerous studies have shown that altering the surface characteristics of PPSU membranes affects their stability and functionality. Nanocomposite membranes of PPSU (P0), PPSU-1%TiO_2 (P1), and PPSU-2% TiO_2 (P2) were prepared using the phase inversion method. Scanning electron microscopy and thermal analysis were performed to determine the contact angle and mechanical integrity of the proposed membranes. The results showed that the membranes contained channels of different diameters extending between 1.8 µm and 10.3 µm, which made them useful in removing oil. Thermal measurements showed that all of the PPSU membranes were stable at a temperature of not less than 240 °C, and had good mechanical properties, including tensile strength of 7.92 MPa and elongation of 0.217%. These properties enabled them to function in a harsh thermal environment. The experimental results of oil and water separation and BSA solution fouling on membrane P2 showed a 92.95% rejection rate and a flux recovery ratio of 82.56%, respectively, compared to P0 and P1.

Keywords: PPSU; TiO_2; nanoparticles; ultrafiltration membrane; oily wastewater treatment; antifouling.

INTRODUCTION

Oily wastewater (OW) is produced by several industrial processes, including petrochemical, chemical, metallurgical, pharmaceutical, textile, steel, leather, and food manufacturing [Ismail et al., 2019; Alsalhy et al., 2016]. Therefore, the produced OW must be appropriately treated to address environmental and human health concerns [Bahmani et al., 2021]. The hydrocarbon content of fresh water sources grows as a result of the growth of these sectors. Free-floating oil (>150 lm), unstable dispersed oil (20–150 lm), and stable emulsion (20 lm) are the three forms of oil that may be found in water [Kong and Li, 1999]. Stable emulsion droplets cannot be removed using conventional methods such as flotation, chemical coagulation, or heat treatment [Ahmad et al., 2013]. Ultrafiltration is one of the various methods being used to treat oily wastewater today [Sun et al., 2018]. Other methods are ultrasonic separation [Stack et al., 2005], adsorption [Soares et al.,

2017], and coagulation/flocculation [Canizares et al., 2008]. However, these methods have disadvantages, such as the need for a large area and the high cost of these procedures. However, because of its unique characteristics such as ease of use and low energy consumption together with the lack of phase transition, membrane processes are considered a viable and cost-effective alternative to traditional methods for treating oilfield wastewater [Ong et al., 2014].

Membrane separation methods have become a widely accepted alternative method for separating oil from water. Microfiltration (MF), ultrafiltration (UF), nanofiltration (NF), and reverse osmosis (RO) are various forms of membrane technology. These membranes have different pore sizes, which is why they have different applications [Pendergast and Hoek, 2011]. Compared to traditional separation processes, UF has low energy cost and high oil removal efficiency without the need to use chemical additives [Alsalhy et al., 2013] .

Sulfone polymers, such as polyphenylsulfone (PPSU), have been extensively investigated for their potential use in membrane science and technology [Nayak et al., 2017]. High thermal and mechanical stability, chemical resistance, impact resistance, and hydrolytic stability are several advantages that PPSU-based membranes offer. PPSU polymers are well-suited for a wide variety of filtration processes, from ultrafiltration to reverse osmosis, because of their bulk modification capability in the polymer's skeleton and the flexibility to customize the pore size of the RO membrane and its porosity [Feng et al., 2016].

Polymeric membranes are increasingly incorporating nanoparticles (NPs) because of their specific characteristics [Salim et al., 2022], functionalization for oily wastewater treatment, and nanoscale size reactivity and large surface area [Lu et al., 2016]. Titanium dioxide (TiO_2), silicon dioxide (SiO_2), aluminum oxide (Al_2O_3), ferrous oxide (Fe_3O_4), carbon nanotubes (CNTs), graphene oxide (GO), zirconium dioxide (ZrO_2), silver (Ag), zinc oxide (ZnO), mobil composition of matter number 41 (MCM-41), and oxygen-deficient tungsten oxide ($WO_{2.89}$) are common inorganic NPs [Waghmode et al., 2019; Haider et al., 2018; Alsalhy et al., 2018; Amna et al., 2020; Aljumaily et al., 2018; Aljumaily et al., 2019; Amna et al., 2020; Rana et al., 2021; Reham et al., 2022]. Inert gas condensation, sol-gel, sputtering, spark discharge, ultrasound, coprecipitation, hydrothermal, and biological processes are applied to manufacture these NPs, which are then integrated into the polymers [Haider et al., 2019]. Additionally, inorganic nanoparticles have been used to enhance the qualities of polymeric membranes, such as antifouling, permeability, and thermal and mechanical stability by incorporating them into the composite membranes [Rahimpour et al., 2008]. TiO_2 is the most common inorganic nanoparticle because of its high hydrophilicity, photocatalytic capabilities, anti-fouling properties, and remarkable chemical and thermal durability. A thin layer of water molecules forms on the surface of TiO_2 because of its superhydrophilicity, which results in high hydration of its surface. The self-cleaning characteristic of TiO_2 is enhanced by its photocatalytic nature, which also helps to keep the surface spotless [Rabiee et al., 2014]. However, the number of nanoparticles (such as TiO_2, SiO_2, and carbon nanotubes) that may be put into the membrane structure before the phase inversion casting process causes considerable changes to the membrane's morphology. Coating membrane surfaces by adding inorganic nanoparticles may be regarded as an efficient alternative method to increase membrane stability, antifouling performance, and separation efficiency [Salim et al., 2021].

Hosseini et al. 2018 reported that 93–99% of 200 ppm oil content is removed by polyethersulfone (PES) TiO_2 NPs. Removal of oil improved when the concentration of the polymer was increased in the casting solution and declined with an increase in the NP amount.

No previous study has been conducted on the PPSU/TiO_2 ultrafiltration (UF) membrane process in oily wastewater treatment. Thus, the present study fills a research gap by incorporating TiO_2 NPs into a PPSU polymer solution at various concentrations. Characterization of PPSU/TiO_2 was conducted using scanning electron microscopy (SEM), contact angle, tensile test, and thermogravimetric analysis (TGA). Furthermore, calculations of pure water flux (PWF), antifouling performance by BSA solution, and removal of oil for each membrane have been analyzed.

MATERIALS AND METHODS

Materials

PPSU (Ultrason P 3010) was supplied by BASF (Berlin, Germany).

N-methyl-2-pyrrolidone (NMP, > 98%) and TiO_2 (<25 nm particle size, 99.7%) were from Sigma-Aldrich. Polyvinylpyrrolidone (PVP, average MW 10,000), sodium azide (99.5%), and methylene blue (MW = 373) were obtained from Sigma-Aldrich (Kenilworth, NJ, USA). Bovine serum albumin (BSA) (MW approximately 69 kDa) was purchased from CDH Chemicals, India.

Preparation of PPSU/TiO_2 membrane

The PPSU membrane was manufactured with a slight modification to the phase inversion technique previously described [Shukla et al. 2017]. Then, 17% PPSU and 1% PVP were dried into 82% NMP for 3 h at 60 °C with moderate stirring. To make the PPSU/TiO_2 nanocomposite membrane, we added 1% and 2% TiO_2 to the PPSU solution and sonicated it for 1 h using a digital sonicator (Branson Ultrasonics, USA) to obtain a transparent homogeneous solution. The evenly distributed TiO_2 NPs were then hand cast onto a clean and dry glass plate with a blade to a thickness of 100 ± 3 µm. For phase inversion, the glass plate was gently immersed in a coagulation bath containing distilled water. The membrane floated to the top of the water in a minute. To avoid microbial contamination, we removed the membrane, cleaned it with DI water, and kept it in an aqueous solution of 0.2% sodium. Details of the prepared membranes are shown in Table 1. The schematic of membrane fabrication is shown in Figure 1.

Characterization

Scanning electron microscopy

The surface and cross-sectional morphology of membranes were studied using SEM (JEOL, Tokyo, Japan). Sputtered Pt coatings were applied to membrane samples having an area of approximately 0.5 cm^2 that were taped to support. Cross-sectional pictures were obtained by orienting the membranes perpendicular to the electron beam. A series of magnifications were made to capture the SEM pictures at a working distance of 6.4 mm and an accelerating voltage of 10 kV.

Table 1. Codes of fabricated membranes

Membrane sample	Membrane code	PPSU (wt.%)	PVP (wt.%)	NMP (wt.%)	TiO_2 (wt.%)
PPSU+ 0% TiO_2	P0	17	1	82	0
PPSU+ 1% TiO_2	P1	17	1	81	1
PPSU+ 2% TiO_2	P2	17	1	80	2

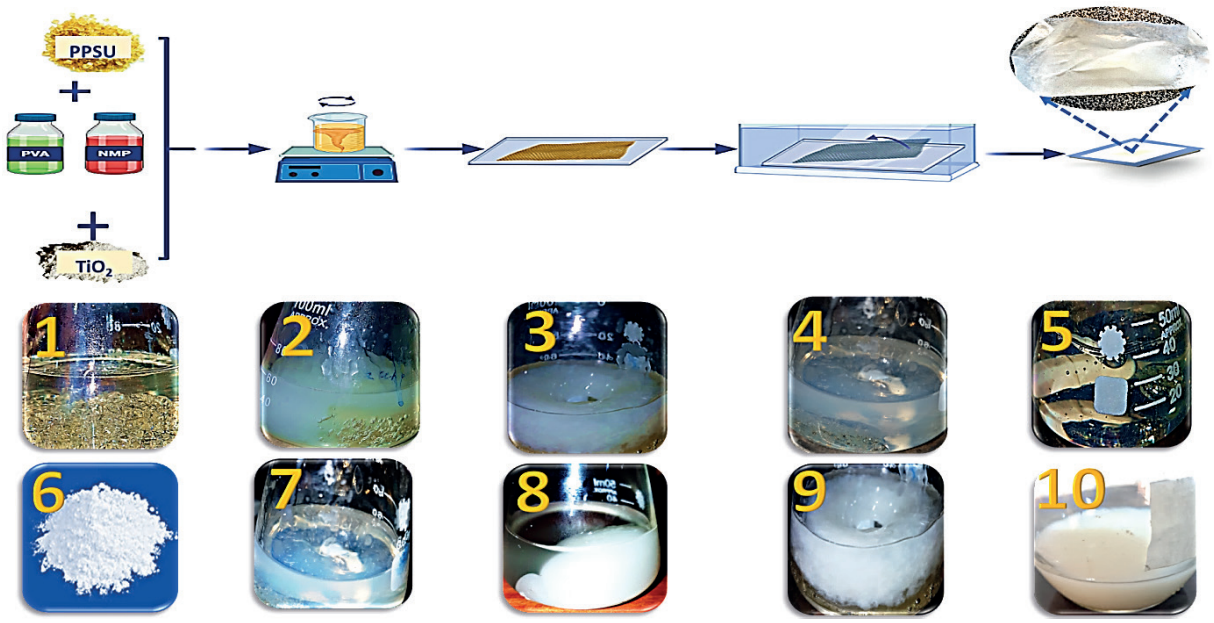

Figure 1. Preparation of polyphenylsulfone (PPSU/TiO_2) membrane

Contact angle measurements

Sessile drop technique was used to measure the hydrophilicity of the membranes. Goniometer (Atension, MAC 200, Biolin Scientific, Amsterdam, Netherlands) coupled with a digital camera and image processing software was used to measure the contact angles of the surfaces. Using a microliter syringe, we deposited water droplets with volumes of 3 1 L at five points on the membrane surface. The digital camera captured a 2D picture of each water droplet's profile on the membrane surface. Contact angles (q) were averaged from five measurements.

Tensile test

A computerized universal testing machine, type D638 was used to perform the tensile test on the samples (WDW-50E). The test was performed at room temperature with a steady strain rate of approximately 5 mm per minute (Vertex 80, Bruker, UK).

Thermogravimetric analysis (TGA)

The temperature ranged from 25 °C to 600 °C for the thermogravimetric analysis of the produced membranes (Veeco, San Jose, CA, USA). A flow rate of 30 mL/min and a heating rate of 10 °C/min were applied in a nitrogen environment. A 6.9012 mg dry sample was used. The sample mass measurement had a standard uncertainty of 1%. Calcium oxalate, delivered along with the device which was used to calibrate it.

PWF of membranes

We determined the water permeability of membranes using a cross-flow filtration cell. Before the experiment, the flat sheet membrane was rinsed with deionized water. In the membrane module, the PPSU flat sheet membrane was sliced into a square sheet with a surface area of 18 cm^2, as illustrated in Figure 2. The module's intake was fitted with a pressure gauge and attached to a feed solution tank. Deionized water was used as the feed solution to estimate the pure water flow, followed by measurements of the permeate water flux utilizing the membrane for 2 h. Permeate was taken from the membrane at regular intervals (30, 45, 60, 75, 90, 105, and 120 min). PWF was calculated by the following equation (1) [Tiron et al., 2017]:

$$Jw1 = \frac{V}{A.T} \tag{1}$$

where: $Jw1 = PWF$ (L/m^2.hr);
V – volume of permeate (L);
T – permeation time (s);
A – membrane surface area (m^2).

Antifouling study of membranes

A 0.5 M phosphate buffer solution (pH 4.0) containing 0.1% BSA solution was used as the feed solution in the fouling investigations. Jw_1 was determined at a transmembrane pressure of 2 bar after the membranes were compressed for 15 min, in accordance with equation (1). Finally,

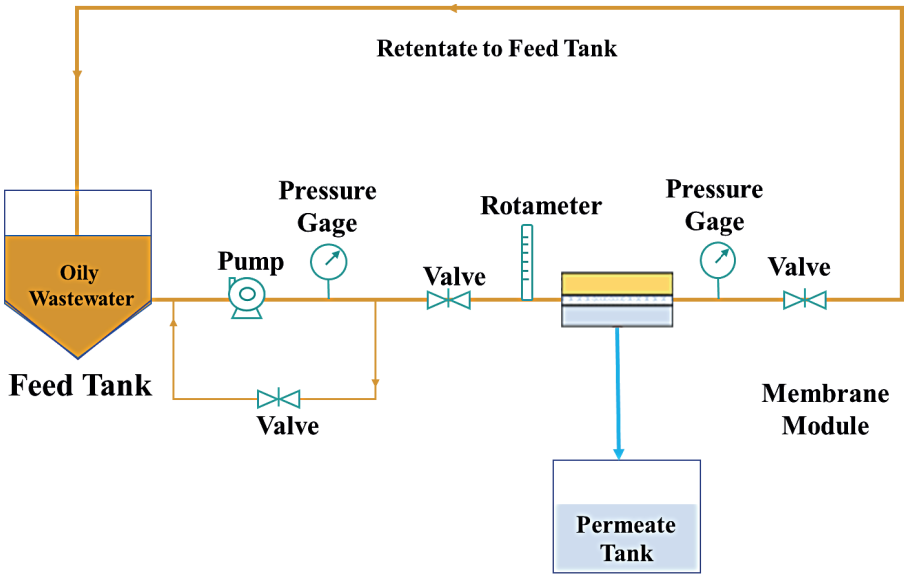

Figure 2. Schematic of ultrafiltration experimental system

the cell was flushed and refilled with a solution of BSA. In the second hour of filtration, the initial protein flow (*Jb*) and steady-state protein solution flux (*Jp*) were measured. The following equations can be used to determine the antifouling properties of the membranes and estimate the fouling resistance for reversible and irreversible protein fouling in filtering processes [Tiron et al. 2017]:

$$Rr(\%) = \frac{Jw2 - Jb}{Jw1} \times 100 \quad (2)$$

$$Rir(\%) = \frac{Jw2 - Jw1}{Jw1} \times 100 \quad (3)$$

where: Jb – permeated flux. The membrane total fouling (Rt %) was calculated by the reversible and irreversible fouling and defined as follows [Tiron et al. 2017]:

$$Rt = Rr + Rir \quad (4)$$

The fouled membrane was washed with deionized water after filtration of the BSA solution for 2 h. The pure water flux, Jw_2, of the cleaned membrane was measured again under the same conditions, and flux recovery ratio (*FRR*) was calculated as follows [Tiron et al. 2017] :

$$FRR\ (\%) = \frac{Jw2}{JW1} \times 100 \quad (5)$$

Procedure for oily wastewater separation and rejection

Oily wastewater was collected from a local refinery in Iraq after the dissolved air flotation (DAF) process. The oil was analyzed in the sanitary laboratory at the University of Technology - Iraq using the gravimetric method. The organic phase was extracted from the aqueous phase using n-hexane as a solvent (EPA method 1664). Three 30 ml parts of n-hexane were used to extract 400 ml of oily water, and one 20 ml piece was used for the final rinse in this phase. An analytic funnel containing filter paper and 10 grams of anhydrous sodium moistened with n-hexane was used to drain the organic phase into an Erlenmeyer flask, where it was collected. The color of the extract in the flask was then examined by placing it on a stirrer plate. Gravimetric analysis was performed using technique A because the extract exhibited a mild yellowish color. The method was performed in the following stages. Magnetic stirring of the Erlenmeyer flask with silica gel (3.0 g) was conducted for 5 min. A round-bottom distillation flask had been reweighed before the extract was filtered and collected. An IKA RV 05 Basic 1-B rotary evaporator was used to remove the solvent from this flask, which was then placed under nitrogen flow for 1 h. After this length of time, the flask was weighed again. At the end of the extraction, the oil rejection R (%) of the oily wastewater was calculated as follows [Tiron et al. 2017]:

$$R(\%) = \left(1 - \frac{\mathrm{Cp}}{\mathrm{Cf}}\right) \times 100 \quad (6)$$

where: Cp and Cf are the concentrations of all parameters in permeate and feed, respectively.

RESULTS AND DISCUSSION

SEM analysis

The morphology of the top surface and cross-section of PPSU/TiO_2 membranes was inspected through SEM as shown in Figure 3.

Figure 3a shows that the top surface of pristine PPSU had a high pore density with very small pore size. Furthermore, Figure 3b shows that the membrane fabricated from pristine PPSU had finger-like channels at the top with randomly distributed macro-voids at the bottom. Furthermore, a sponge layer can be observed as an essential layer of the cross-section because of the moderately high viscosity of the casting mixture caused by the high polymer concentration (17 wt.% PPSU).

Adding TiO_2 with 1 wt.% and 2 wt.% to the casting solution resulted in good optimal dispersion of titanium oxide in the membrane matrix, thereby modifying the morphology of the PPSU membrane. In addition, it led to an increased solubility factor between the solvent and the non-solvent, resulting in the elimination of macro-voids, and thus the formation of a highly porous or dense structure (Figures 3d and 3f). The top surface of the fabricated membranes P1 and P2 had higher pore density with smaller pore size than the top surface of the P0 membrane (Figures 3c and 3e).

Analysis of contact angle and thickness

The contact angle is often measured to determine the types of suitable materials and ensure

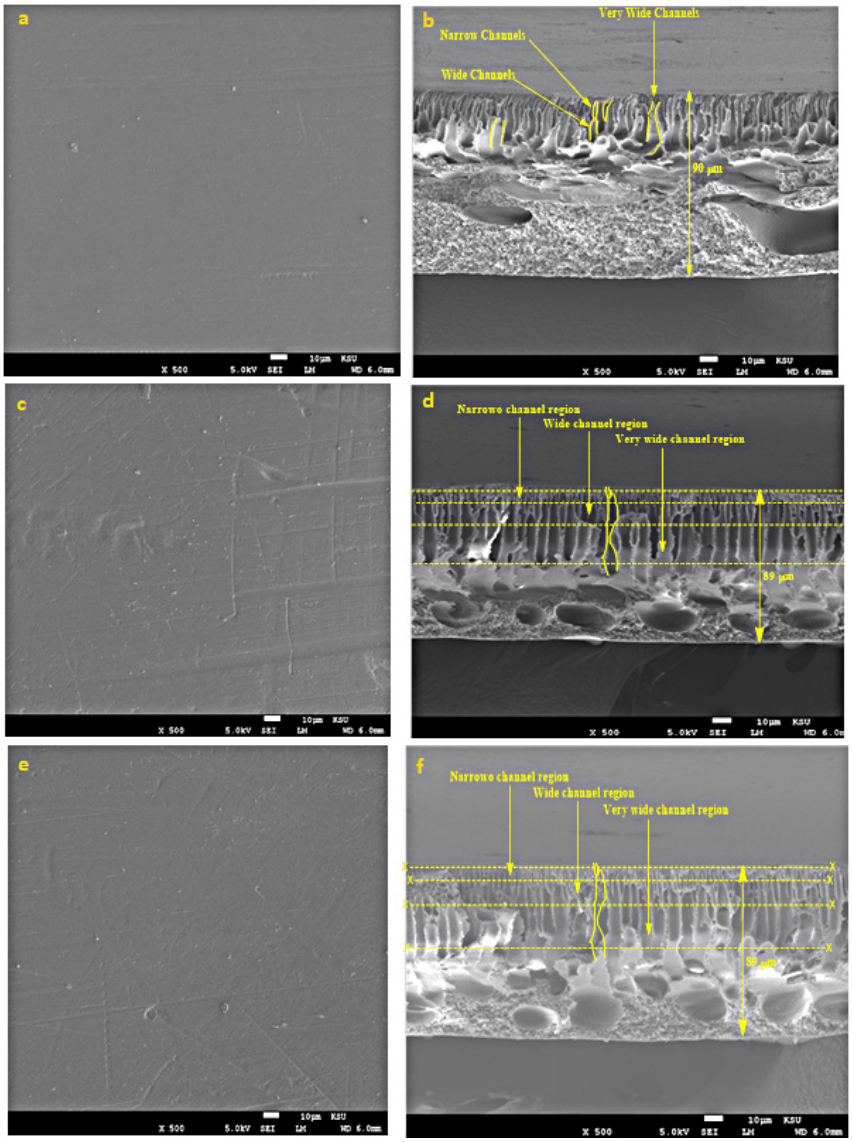

Figure 3. SEM image of three used membranes: P0 (a, b), P1 (c, d), and P2 (e, f) (left: top surface and right: cross section)

the optimum use of the fabricated membranes. On the basis of hydrophilicity and hydrophobicity, the membranes can be classified as those used for removal of water-based pollutants and those used for removal of organic pollutants. Figure 4 (top) shows that the prepared membranes have contact angles of 69°, 65°, and 64° for P0, P1, and P2, respectively. The contact angle after adding nano-titanium oxide became lower, which means that the surface area increased and the contact angle decreased. This condition enhanced the possibility of using the membrane to remove organic and inorganic pollutants, and thus, the membrane achieves a high probability of use in different applications [Taylor et al. 2007]. Furthermore, membrane thickness of P0, P1, and P2 was observed by SEM and summarized in Figure 4 (bottom). The thickness of all the membranes was approximately similar.

Tensile test analysis

The stress–strain curve (Fig. 5) shows that the P0 polymer and P1 is a ductile and not a brittle material, where the tensile strength value is equal to 7.318 MPa and the elongation value is 0.261% [Xu, 2019]. In the case of P2, the tensile strength value was increased and found to be 7.92 MPa, while the elongation value was 0.217%. The measurement proves that 1% addition of TiO_2 NPs did not cause a significant change in the mechanical properties of the membrane. However, a significant change was observed when the amount of TiO_2 was increased by 2%.

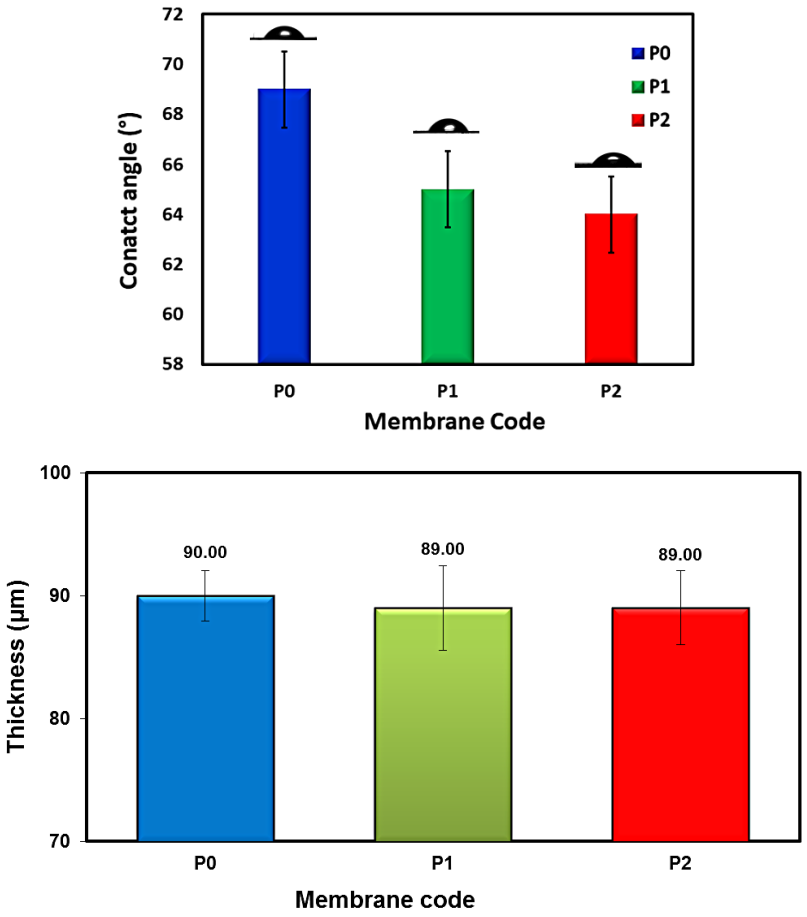

Figure 4. (Top) contact angle and (bottom) membrane thickness

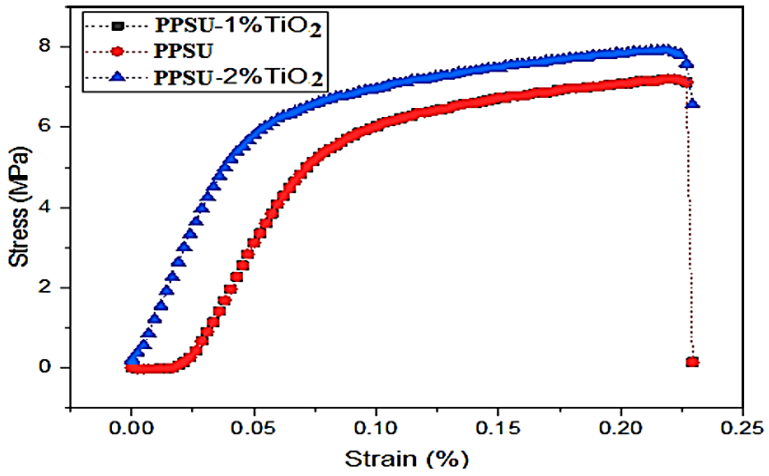

Figure 5. Stress–strain curve of P0, P1, and P2

Thermogravimetric analysis

To ascertain the thermal stability of the polymeric membrane, we took 0.6944 grams of it and placed it on a platinum pan in the thermal analyzer. The weight loss stages were recorded at different temperatures. A temperature of 50–240 °C indicated a loss of approximately 57%, 42%, and 37% of the total weight of the PPSU, PPSU -1%TiO_2, and PPSU -2%TiO_2 membranes, respectively. This stage was due to the beginning of polymer melting. At 240–750 °C, a loss of approximately 79%, 78%, and 68% of the total weight of the PPSU, PPSU -1%TiO_2, and PPSU -2%TiO_2, respectively, was observed as a result of the decomposition of chemical bonds. At

1,000 °C, breakdown of the rest of the polymer and its transformation into gas resulted from combustion [Hatakeyama et al. 1999]. The results showed that all membranes were stable for use even when their composition was not changed to 240 °C. Therefore, the membranes have potential to be used in applications where heat is essential. Figure 6 shows that increasing the percentage of TiO_2 increases the stability of the polymer because weight loss is least possible for the membrane containing 2% of TiO_2.

PWF

Nanocomposite membranes P1 and P2 enhanced water permeability compared to the P0 membrane (Fig. 7), notably with increasing TiO_2 concentration from 1.0% to 2.0%. The water permeability increased to twice that of the pristine membrane P0. The average PWF for P0, P1, and P2 were 35.03, 45.75, and 54.53 L/m^2·hr. The increasing water flux was also due to the presence of PVP as a pore-forming additive that affected the morphology of the PPSU membrane and increased the water flux [Nayak et al. 2017].

Antifouling study

A common problem with membranes is fouling, which reduces their ability to separate and increases their energy consumption. The antifouling capabilities of the TiO_2-modified membrane were evaluated by monitoring water flux recovery following BSA solution fouling. Fouling may be influenced by various factors, including the solute-membrane interface, polymer chemical and structural characteristics, ionic strength, and pH [Shi, 2016]. Table 2 shows the calculated FRR, Rr, and Rir fouling ratios (reversible and irreversible, respectively). Using the FRR metric, the antifouling

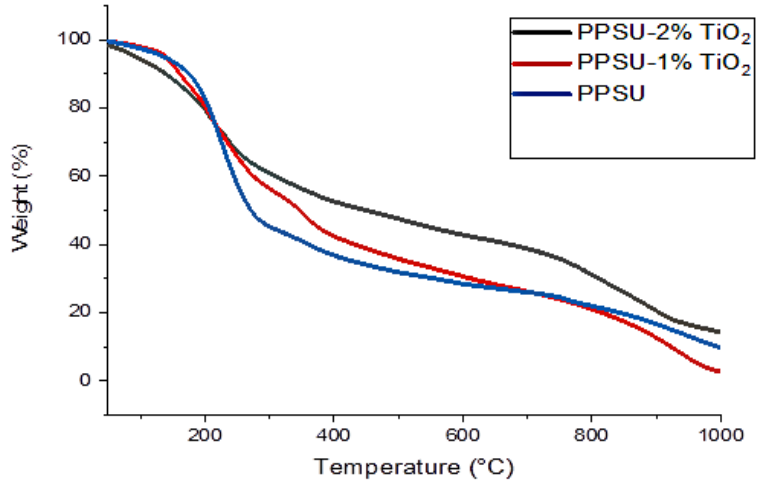

Figure 6. Thermal analysis of P0, P1, and P2

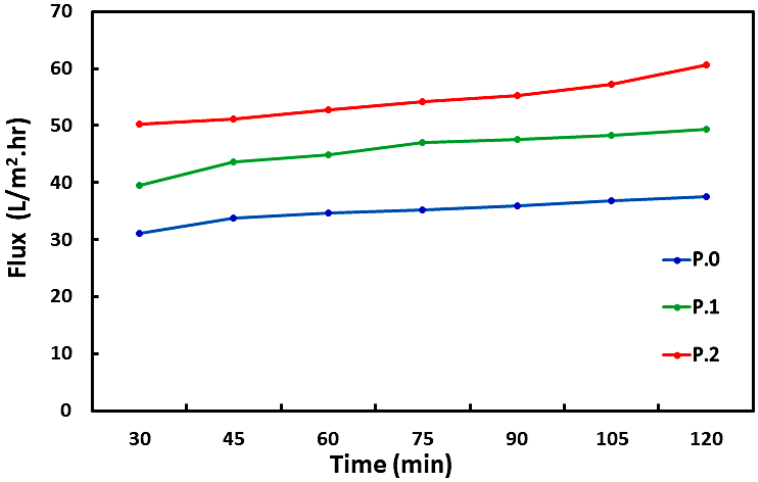

Figure 7. Time-dependent pure water flux of membranes

Table 2. Permeation flux of membranes and antifouling results

Membrane code	J_{w1} (L/m²·hr)	J_p (L/m²·hr)	J_{w2} (L/m²·hr)	*FRR* (%)	R_r	R_{ir}	R_t
P0	35.03	11.20	28.35	80.94	48.96	19.06	68.02
P1	45.75	14.61	37.25	81.43	49.49	18.57	68.06
P2	54.53	16.49	45.02	82.56	52.33	17.44	69.77

capabilities of the modified membranes may be assessed, and P2 had an FRR of 82.56%. The FRR value improved when TiO_2 nanoparticles were added to the membrane, according to the data. Hydrophilic TiO_2 particles minimized the fouling of PPSU/TiO_2 membranes due to the presence of hydrophilic groups (hydroxyl and amine) on its surface, which led to the production of a thin water layer on the membrane surface and enabled cleaning. Water molecules and hydrophilic groups on the nanoparticles exposed to the feed solution on the membrane surface showed more intense interaction, thereby reducing membrane fouling [Cheshomi et al. 2018].

As shown in Figure 8, PPSU surface modification using TiO_2 nanoparticles was shown to be an efficient method for increasing the water flow and antifouling capabilities of the membranes, according to the findings of this study.

The resulting hydrophilic particle layer acts as a hydrophilic filtration membrane in isolating pollutants and supporting membranes from

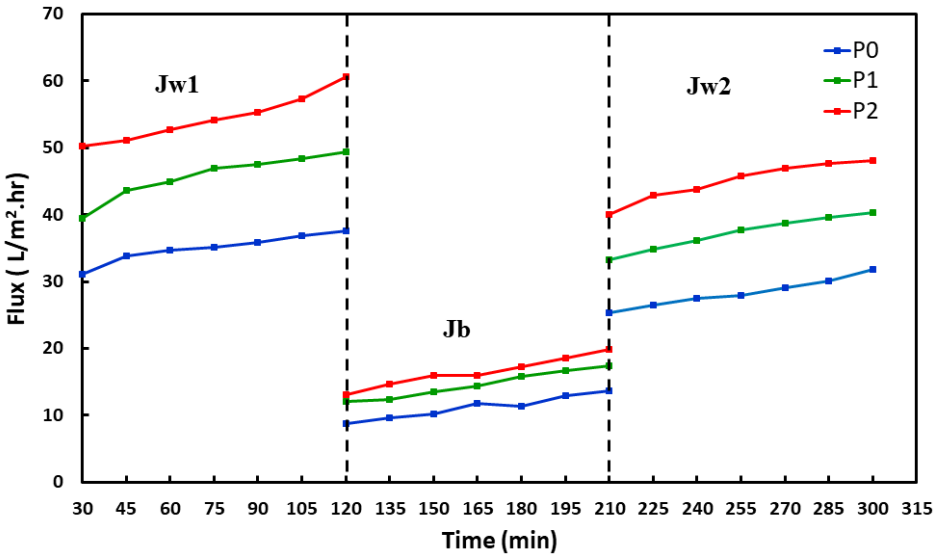

Figure 8. Antifouling analysis on P0, P1, and P2 membranes using BSA as model foulant

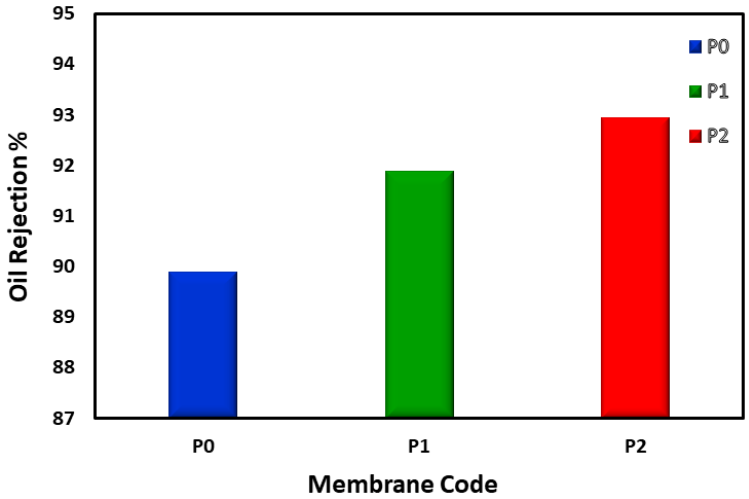

Figure 9. Oil in water separation results in membranes

Table 3. Comparison between performance of membranes prepared in this study with various membranes found in the literature in terms of total pure water flux and removal efficiency

Polymer type	Polymer concentration	Operating pressure/ Transmembrane pressure	Nanoparticles		Contact angle	Removal efficiency (%)	Pollutants type	PWF ($L/m^2 \cdot h$)	Reference
			Type	Concentration wt%					
PES*	17 wt%	1 to 4 bar	Carboxylated-MWCNTs	0.1	70° to 80°	67 & 85	Bromothymol blue (BTB) and methyl orange (MO)	20	[Hosseini et al.2018]
PVC*	15 wt%	1 to 7.4 bar	TiO_2	0.5 1 1.5	62.5°	96.3	Oil and grease	116	[Shukla et al. 2017]
Ceramic			CuO-TiO_2	--	--	99.5	Ciprofloxacin	--	[Tiron et al. 2017]
PES*	18 wt%	0.3 MPa	ZnO	1 2	61.3° 60.5°	98	Bovine serum albumin (BSA)	748.1	[Taylor et al. 2007]
PES*	19 wt.%	5 bar	$WO_{2.89}$	0 0.1 0.2 0.3	68.18° 63° 62° 61.4°	86	Congo red (CR)	54.9	[Xu 2019]
PSF*	18 wt.%	5 bar	SiO_2	0 1 2 3 4	78.3° 69.7° 52.5° 43.2° 45.8°	89.81	Amoxicillin	42.28	[Hatakeyama et al. 1999]
PAN*	15–18 wt.%	1 bar	Goethite	0.0 0.1 0.3 0.5	66.7±0.4° 46.5±0.4° 40.2±1.7° 38.8±0.1°	49.1	Copper	240	[Shi 2016]
PES*	18 wt.%	4 bar	g-C_3N_4	---	52.13°	35.78	Phenol	55.50	[Cheshomi et al. 2018]
PVDF*	16 wt%		UiO-66-NH_2	0.02	90.16°	99 85.58	Cr (VI) Cr (III)	561	[Lu et al. 2018]
PES*	16 wt%	1 bar	$ZnFe_2O_4$	4	52°	94 96	HA oil/water emulsion	687	[Shukla et al. 2020]
PSF*	10 wt%	4-6 bar	CNTs	0, 5 10	--	99.9	Oil separation	190	[Al-Ani et al. 2020]
PEI*	18 wt%	0.2 MPa	GO	0–0.3	39.62±2.5°	95.5 92.4	Ni^{2+} Cd^{2+}	101.5±10	[Bhattacharya et al. 2019]
PSF/PES*	% of 25:75 PSF/PES	100-300 kPa	CNT	0.5 1 1.5	--	55.6 13.5	Phenol and benzene	309	[Nasrollahi et al. 2018]
PES*	18.52–20.00 wt%	2.5 bar	Fe-MOF	0 2 4 6 8	85.49° 78.89° 72.77° 69.57° 78.82°	>98.5	Cationic and anionic dyes	165.68	[Abdullah et al. 2022]
PES*		1 bar	HAp/AC	0 0.5 1 2 4	69° 63° 55° 57.5° 42°	93.7 98.6	Humic acid (HA) Bovine serum albumin (BSA)	540	[Shakak et al. 2020]
PAI*	16.75–17.5 wt%	345 kPa	MoS_2	0.5 0.75	70.1° 66.8°	95.8 93.2	Bovine serum albumin (BSA) Humic acid (HA)	105.6	[Zahed et al. 2018]
PVDF*	2 wt.%	0.05−0.35 MPa	Al_2O_3 SiO_2 CuO Verm	0.2 0.3 0.1 0.2	62.45° 64.75° 66.42° 57.25°	87 80 85 89	Malachite green (MG)	598 590 585 628.7	[Salimet al. 2019]
PSF*	18 wt%	0.2 MPa	SiMo	0.3	42.2° ± 2.55°	99	Bovine serum albumin (BSA)	80	[Zhang et al. 2021]
Cellulose acetate	17.5 wt%	345 kPa	HMO	0 0.25 0.5 1	93.6° 81.7° 75° 61.3°	95.9	Bovine serum albumin (BSA)	143.6	[Kallem et al. 2021]
PSF/PVA*	Ratio of 80:20	1 bar	ZnO	0.2 0.5	43.3° 41.8°	53.5	Congo red dye	26	[Maphutha et al. 2013]
PVDF	19 wt%	0.1 MP	Al_2O_3	1 2	--	90%	Oily wastewater	138.53	[Kaleekkal et al. 2017]
PES PVDF PTFE	Commercial PES, PVDF, and modified PVDF membranes	0.1 MPa	TiO_2 TiO_2/CNT composite	--	55.9±0.8° 57.2±0.6° 105.5±2.5°	83–91 >98 >98	Contaminated oil	301–362	[Rameetse et al. 2020]
PES	15 wt.%	1 bar	TiO_2 HMO	--	44.1° 47.1°	94.5–99.6	Oily wastewater	57 40	[Johari et al. 2021]
PPSU	22 wt.%	6 bar	ZnO	0, 0.01 0.015 0.02 0.025 0.03	77.5 67 60 57 48	--	--	107	[Pendergast and Hoek 2011]
PPSU*	17 wt.%	2 bar	TiO_2	1 2	65° 64°	91.88, 92.95	Oily wastewater	45.75 54.53	The current work

Note: *PVDF: polyvinylidene fluoride, PTS/PSF: phosphorylated/polysulfone, PD: polydopamine PVC: polyvinyl chloride, PES: polyethersulfone, PPSU: polyphenylsulfone, PSF: polysulfone, PNA: polyacrylonitrile, CNTs: carbon nanotube, GO: graphene oxide, Fe-MOF: ferric-based metal-organic framework, HAp/AC: hydroxyapatite-decorated activated carbon, and PAI: polyamide-imide.

fouling. The membranes exhibit increased permeate flux resistance depending on particle size (a larger particle size produces dynamic membranes with lower resistance) [Lu et al. 2018]. Backwash can easily remove particles in the dynamic membrane because they are not chemically bonded to one another or to the supporting membrane. As a result, fouling on the membrane is reversible. Furthermore, the membrane can be regenerated after backwashing by applying another hydrophilic particle layer. As a result, PPSU-TiO_2-NP membranes have the advantages of easy preparation and regeneration.

Oil rejection

Increases in TiO_2 additives and PVP as a pore forming agent resulted in improved membrane oil rejection efficiency. In this study, only water molecules passed through the membrane and produced oil-free water after the oil droplets were rejected on the membrane surface. Figure 9 shows that membranes P2, P1, and P0 have 92.95%, 91.88%, and 89.90% rejection rates, respectively.

COMPARATIVE STUDY

Table 3 shows a comparison between the performance of membranes prepared in this study with various membranes found in the literature. The comparison was according to the removal efficiency and total pure water flux. The PPSU-TiO_2-NP membranes have a reasonable pollutant removal efficiency and PWF compared with most membranes in previous research.

CONCLUSION

Several applications of membrane technology have been used, such as water purification and desalination, as well as oily wastewater treatment, because they are simple and fast to perform. Up to this point, most of the research has focused on the development of new membranes. Oil and water separation is a vital stage, but a study on the process and the mechanisms by which the oil droplets are rejected on the membrane surface is limited. Phase inversion was effectively performed to manufacture polymeric membranes for the treatment of oily effluent from a local refinery in Iraq. Thermal analysis, contact angle, and SEM determined the capabilities of the produced membranes. Changes in membrane morphology and pore size distribution occurred as a result of adding TiO_2 nanoparticles to the PPSU membranes. The hydrophilicity and PWF properties of PPSUs were improved when TiO_2 NP concentrations in the casting solution were increased. The P2 membrane had a higher FRR of 82.56%. Using BSA as the model foulant indicated a higher antifouling capacity. A rejection of 92.95% was observed for membrane P2, whereas 91.88% and 89.90% rejection rates were found in the oil-in-water separation experiments performed on membranes P0 and P1. The SEM images showed that the channels between the membranes provided a good water penetration route. The findings of this study are expected to pave the way for large-scale antifouling membranes based on TiO_2 NPs that can be used in a wide range of water treatment applications.

REFERENCES

1. Abdullah R.R., Shabeed, K.M., Alzubaydi A.B., Alsalhy, Q.F. 2022. Novel photocatalytic polyether sulphone ultrafiltration (UF) membrane reinforced with oxygen-deficient Tungsten Oxide (WO2. 89) for Congo red dye removal. Chemical engineering research and design, 177, 526–540.
2. Ahmad A.L., Abdulkarim A.A., Ooi B.S., Ismail S. 2013. Recent development in additives modifications of polyethersulfone membrane for flux enhancement, Chem. Eng. J., 223, 246–267.
3. Al-Ani F.H., Alsalhy Q.F., Raheem R.S., Rashid K.T., Alberto F.I. 2020. Experimental investigation of the effect of implanting tio2-nps on pvc for long-term uf membrane performance to treat refinery wastewater. Membranes (Basel), 10(4), 77.
4. Aljumaily M., Alsaadi Hashim N.A., Alsalhy Q.F., Das R., Mjalli F.S. 2019. Embedded high-hydrophobic CNMs prepared by CVD technique with PVDF-co-HFP membrane for application in water desalination by DCMD, Desalination and Water Treatment, 142, 37–48.
5. Aljumaily M., Alsaadi N.A., Alsalhy Q.F., Mjalli F.S., Atieh M.A. 2018. PVDF-co-HFP/superhydrophobic acetylene-based nanocarbon hybrid membrane for seawater desalination via DCMD. Chemical Engineering Research and Design, 138, 248–259.
6. Alsalhy Q.F., Ali J.M., Abbas A.A., Rashed A., Bruggen B.V., Balta S. 2013. Enhancement of poly (phenyl sulfone) membranes with ZnO nanoparticles," Desalin. Water Treat., 51(31–33), 6070–6081. DOI: 10.1080/19443994.2013.764487

7. Alsalhy Q.F., Al-Ani F.H., Al-Najar A.E. 2018. A new Sponge-GAC-Sponge membrane module for submerged membrane bioreactor use in hospital wastewater treatment. Biochemical Engineering Journal, 133, 130–139.
8. Alsalhy Q.F., Riyadh S., Almukhtar, Harith A., Al-ani. 2016. Treatment of oil refinery wastewater by membrane bioreactor (MBR), Arabian J. of Sci. and Eng., 41, 2439–2452.
9. Amna J.S., Eman S.A., Kadhum M.Sh., Bassam I.Kh., Sama M., Sabirova T.M., Tretyakova N. A., Hasan S.M., Alsalhy Q.F., Auda J.B. 2020. Comparative study of embedded functionalised MWCNTs and GO in Ultrafiltration (UF) PVC membrane: interaction mechanisms and performance, International Journal of Environmental Analytical Chemistry.
10. Amna J.S., Kadhum M.S., Bassam I.K., Alsalhy Q.F. 2020. Effect of embedding MWCNT-g-GO with PVC on the performance of PVC membranes for oily wastewater treatment. Chemical Engineering Comunications, 207(6), 733–750.
11. Bahmani M., Zarghami S., Mohammadi T., Asadi A.A., Khanlari, S. 2021. PES electrospun fibrous membrane for oily wastewater treatment: Fabrication condition optimization using response surface methodology. Polym. Adv. Technol., 32(2), 886–899. DOI: 10.1002/pat.5140
12. Bhattacharya P., Mukherjee D., Dey S., Ghosh S., Banerjee S. 2019. Development and performance evaluation of a novel CuO/TiO_2 ceramic ultrafiltration membrane for ciprofloxacin removal. Materials Chemistry and Physics, 229, 106–116.
13. Canizares P., Martínez F., Jiménez C., Sáez C., Rodrigo M. A.2008. Coagulation and electrocoagulation of oil-in-water emulsions. J. Hazard. Mater., 151(1), 44–51.
14. Cheshomi N., Pakizeh M., Namvar-Mahboub M. 2018. Preparation and characterization of TiO2/Pebax/(PSf-PES) thin film nanocomposite membrane for humic acid removal from water. Polym. Adv. Technol., 29(4), 1303–1312.
15. Feng Y. 2016. Rheology and phase inversion behavior of polyphenylenesulfone (PPSU) and sulfonated PPSU for membrane formation. Polymer (Guildf)., 99, 72–82.
16. Haider A.J., Al-Anbari R., Sami H.M., Haider M.J. 2019. Photocatalytic Activity of Nickel Oxide. J. Mater. Res. Technol., 8(3), 2802–2808. DOI: 10.1016/j.jmrt.2019.02.018
17. Haider A., Al-Anbari R., Kadhim G., Jameel Z. 2018. Synthesis and photocatalytic activity for TiO2 nanoparticles as air purification. 2018 MATEC Web Conf., 162, 1–6. DOI: 10.1051/matecconf/201816205006
18. Hatakeyama T., Quinn F.X. 1999. Thermal analysis: fundamentals and applications to polymer science.
19. Hosseini S.S., Fakharian T.S., Alaei S.M.A., Tavangar T. 2018. Fabrication, characterization, and performance evaluation of polyethersulfone/TiO_2 nanocomposite ultrafiltration membranes for produced water treatment. Polymers for Advanced Technologies, 29(10), 2619–2631.
20. Ismail N. H.2020. Hydrophilic polymer-based membrane for oily wastewater treatment: A review. Sep. Purif. Technol., 233, 116007. DOI: 10.1016/j.seppur.2019.116007
21. Johari N.A., Yusof N., Lau W.J., Abdullah N., Salleh W.N.W., Jaafar J., Ismail A.F. 2021. Polyethersulfone ultrafiltration membrane incorporated with ferric-based metal-organic framework for textile wastewater treatment. Separation and Purification Technology, 270, 118819.
22. Kaleekkal N.J., Thanigaivelan A., Rana D., Mohan D. 2017. Studies on carboxylated graphene oxide incorporated polyetherimide mixed matrix ultrafiltration membranes. Materials Chemistry and Physics, 186, 146–158.
23. Kallem P., Othman I., Ouda M., Hasan S. W., Al-Nashef I., Banat F. 2021. Polyethersulfone hybrid ultrafiltration membranes fabricated with polydopamine modified $ZnFe_2O_4$ nanocomposites: Applications in humic acid removal and oil/water emulsion separation. Process Safety and Environmental Protection, 148, 813–824.
24. Kong J., Li K. 1999. Oil removal from oil-in-water emulsions using PVDF membranes. Sep. Purif. Technol., 16(1), 83–93.
25. Lu D. 2016. Hydrophilic Fe_2O_3 dynamic membrane mitigating fouling of support ceramic membrane in ultrafiltration of oil/water emulsion. Sep. Purif. Technol., 165, 1–9.
26. Lu H., Wang J., Stoller M., Wang T., Bao Y., Hao H. 2016. An overview of nanomaterials for water and wastewater treatment. Adv. Mater. Sci. Eng.
27. Maphutha S., Moothi K., Meyyappan M., Iyuke S.E. 2013. A carbon nanotube-infused polysulfone membrane with polyvinyl alcohol layer for treating oil-containing waste water. Scientific reports, 3(1), 1–6.
28. Nasrollahi N., Aber S., Vatanpour V., Mahmoodi N.M. 2018. The effect of amine functionalization of CuO and ZnO nanoparticles used as additives on the morphology and the permeation properties of polyethersulfone ultrafiltration nanocomposite membranes. Composites Part B: Engineering, 154, 388–409.
29. Nayak M.C., Isloor A.M., Moslehyani A., Ismail A.F. 2017.Preparation and characterization of PPSU membranes with BiOCl nanowafers loaded on activated charcoal for oil in water separation. J. Taiwan Inst. Chem. Eng., 77, 293–301.
30. Ong C.S., Lau W.J., Goh P.S., Ng B.C., Ismail A.F. 2014.Investigation of submerged membrane photocatalytic reactor (sMPR) operating parameters

during oily wastewater treatment process, Desalination, 353, 48–56.

31. Pendergast M.M., Hoek E.M.V. 2011. A review of water treatment membrane nanotechnologies. Energy Environ. Sci., 4(6), 1946–1971. DOI: 10.1039/c0ee00541j
32. Rabiee H., Farahani M.H.D.A., Vatanpour V. 2014. Preparation and characterization of emulsion poly (vinyl chloride) (EPVC)/TiO2 nanocomposite ultrafiltration membrane. J. Memb. Sci., 472, 185–193.
33. Rahimpour A., Madaeni S.S., Taheri A.H., Mansourpanah Y. 2008.Coupling TiO2 nanoparticles with UV irradiation for modification of polyethersulfone ultrafiltration membranes. J. Memb. Sci., 313(1–2), 158–169.
34. Rameetse M.S., Aberefa O., Daramola M.O. 2020. Effect of loading and functionalization of carbon nanotube on the performance of blended polysulfone/polyethersulfone membrane during treatment of wastewater containing phenol and benzene. Membranes, 10(3), 54.
35. Rana J.K., Al-Ani Faris H., Alsalhy Q.F. 2021. MCM-41 mesoporous modified polyethersulfone nanofiltration membranes and their prospects for dyes removal, International Journal of Environmental Analytical Chemistry, 1–21.
36. Reham R.A., Kadium M.S., Aseel B., Alsalhy Q.F. 2022. Novel photocatalytic polyether sulphone ultrafiltration (UF) membrane reinforced with oxygen-deficient Tungsten Oxide (WO2.89) for Congo red dye removal, Chemical Engineering Research and Design, 177, 526–540.
37. Salim S.H., Al-Anbari R.H., Haider A. 2022. Polysulfone/TiO_2 Thin Film Nanocomposite for Commercial Ultrafiltration Membranes," J. Appl. Sci. Nanotechnol., 2(1), 80–89. DOI: 10.53293/jasn.2022.4528.1121
38. Salim S.H., Al-Anbari R.H., Haider A. 2021. Polymeric Membrane with Nanomaterial's for Water Purification: A Review," in IOP Conference Series: Earth and Environmental Science, 779(1), 12103.
39. Salim N.E., Nor N.A.M., Jaafar J., Ismail A.F., Qtaishat M.R., Matsuura T., Yusof N. 2019. Effects of hydrophilic surface macromolecule modifier loading on PES/Og-C3N4 hybrid photocatalytic membrane for phenol removal. Applied Surface Science, 465, 180–191.
40. Shakak M., Rezaee R., Maleki A., Jafari A., Safari M., Shahmoradi B., Lee, S.M. 2020. Synthesis and characterization of nanocomposite ultrafiltration membrane (PSF/PVP/SiO2) and performance evaluation for the removal of amoxicillin from aqueous solutions. Environmental Technology & Innovation, 17, 100529.
41. Shi H. 2016.A modified mussel-inspired method to fabricate TiO_2 decorated superhydrophilic PVDF membrane for oil/water separation. J. Memb. Sci., 506, 60–70.
42. Shukla A.K., Alam J., Alhoshan M., Dass L.A., Muthumareeswaran M.R. 2017.Development of a nanocomposite ultrafiltration membrane based on polyphenylsulfone blended with graphene oxide. Sci. Rep., 7(1), 1–12.
43. Shukla A.K., Alam J., Alhoshan M., Aldalbahi A. 2020. A facile approach for elimination of electroneutral/anionic organic dyes from water using a developed carbon-based polymer nanocomposite membrane. Water, Air, Soil Pollut., 231(3), 1–16.
44. Soares S.F., Rodrigues M.I., Trindade T., Daniel-da-Silva A.L. 2017.Chitosan-silica hybrid nanosorbents for oil removal from water. Colloids Surfaces a Physicochem. Eng. Asp., 532, 305–313.
45. Stack L.J., Carney P.A., Malone H.B., Wessels T.K. 2005.Factors influencing the ultrasonic separation of oil-in-water emulsions. Ultrason. Sonochem., 12(3), 153–160.
46. Sun S., Xiao Q.-R., Zhou X., Wei Y.-Y., Shi L., Jiang Y. 2018. A bio-based environment-friendly membrane with facile preparation process for oil-water separation. Colloids Surfaces A Physicochem. Eng. Asp., 559, 18–22.
47. Taylor M., Urquhart A.J., Zelzer M., Davies M.C., Alexander M.R. 2007. Picoliter water contact angle measurement on polymers. Langmuir, 23(13), 6875–6878.
48. Tiron L.G., Pintilie C., Vlad M., Birsan I.G., Baltă. 2017. Characterization of Polysulfone Membranes Prepared with Thermally Induced Phase Separation Technique. IOP Conf. Ser. Mater. Sci. Eng., 209(1). DOI: 10.1088/1757-899X/209/1/012013
49. Waghmode M.S., Gunjal A.B., Mulla J.A., Patil N.N., Nawani N.N. 2019. Studies on the titanium dioxide nanoparticles: Biosynthesis, applications and remediation. SN Appl. Sci., 1(4), 1–9.
50. Xu X. 2019.Nanofiltration membrane constructed by tuning the chain interactions of polymer complexation. J. Memb. Sci., 580, 289–295.
51. Zahed S.S.H., Khanlari S., Mohammadi T. 2019. Hydrous metal oxide incorporated polyacrylonitrile-based nanocomposite membranes for Cu (II) ions removal. Separation and Purification Technology, 213, 151–161.
52. Zhang Y., Xu X., Yue C., Song L., Lv Y., Liu F., Li A. 2021. Insight into the efficient co-removal of Cr (VI) and Cr (III) by positively charged UiO-66-NH2 decorated ultrafiltration membrane. Chemical Engineering Journal, 404, 126546.